UNIVERSITY OF ALASKA FAIRBANKS

URSIGA2008
Paper 1536

Whistler Mode Sounding of the Magnetosphere: Measurement of Electron Density, Ion Composition (H+, He+, O+), and Density Irregularities Along the Geomagnetic Field

V. S. Sonwalkar[1], A. Reddy[1], D. L. Carpenter[2], B. W. Reinisch[3]

1) Electrical and Computer Engineering Department, University of Alaska Fairbanks, AK 99775, USA 2) Electrical Engineering Department, Stanford University, CA 94305, USA 3) Center for Atmospheric Research, University of Massachusetts at Lowell, MA 01845, USA

OUTLINE OF THE TALK

- Introduction to whistler-mode (WM) radio sounding by RPI* on IMAGE
- Observations and interpretation of whistler mode echoes
- Measurement of electron, H+, He+, and O+ densities and field-aligned irregularities (FAI) along **B**
- Summary and conclusions

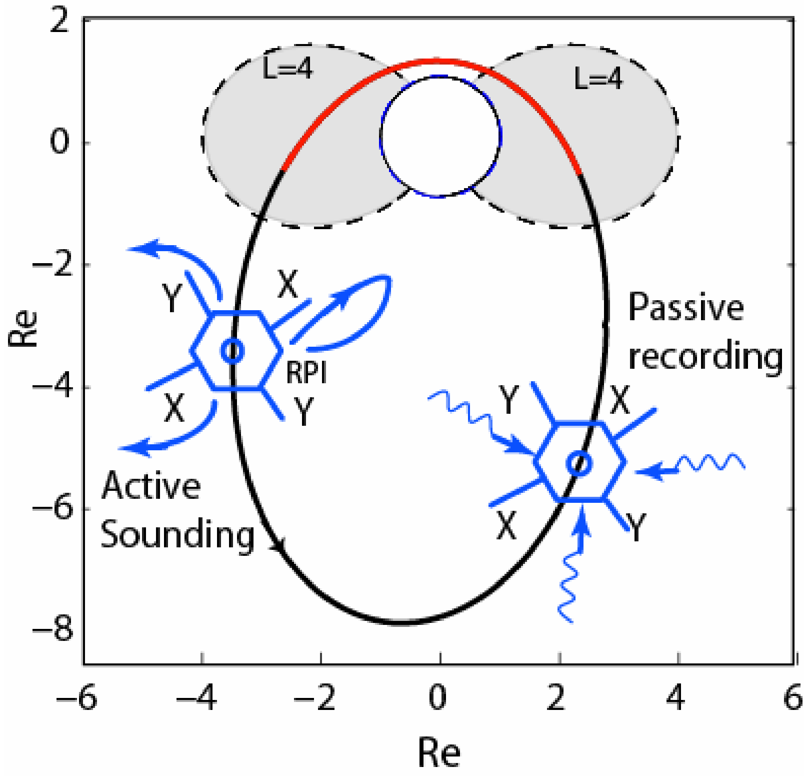

* Reinisch et al. (2000), The Radio Plasma Imager Investigation on Image Spacecraft, *Space Sci. Rev.*, 91, 319

Advantages of Whistler Mode Sounding over R-X, L-O, and Z-mode Sounding

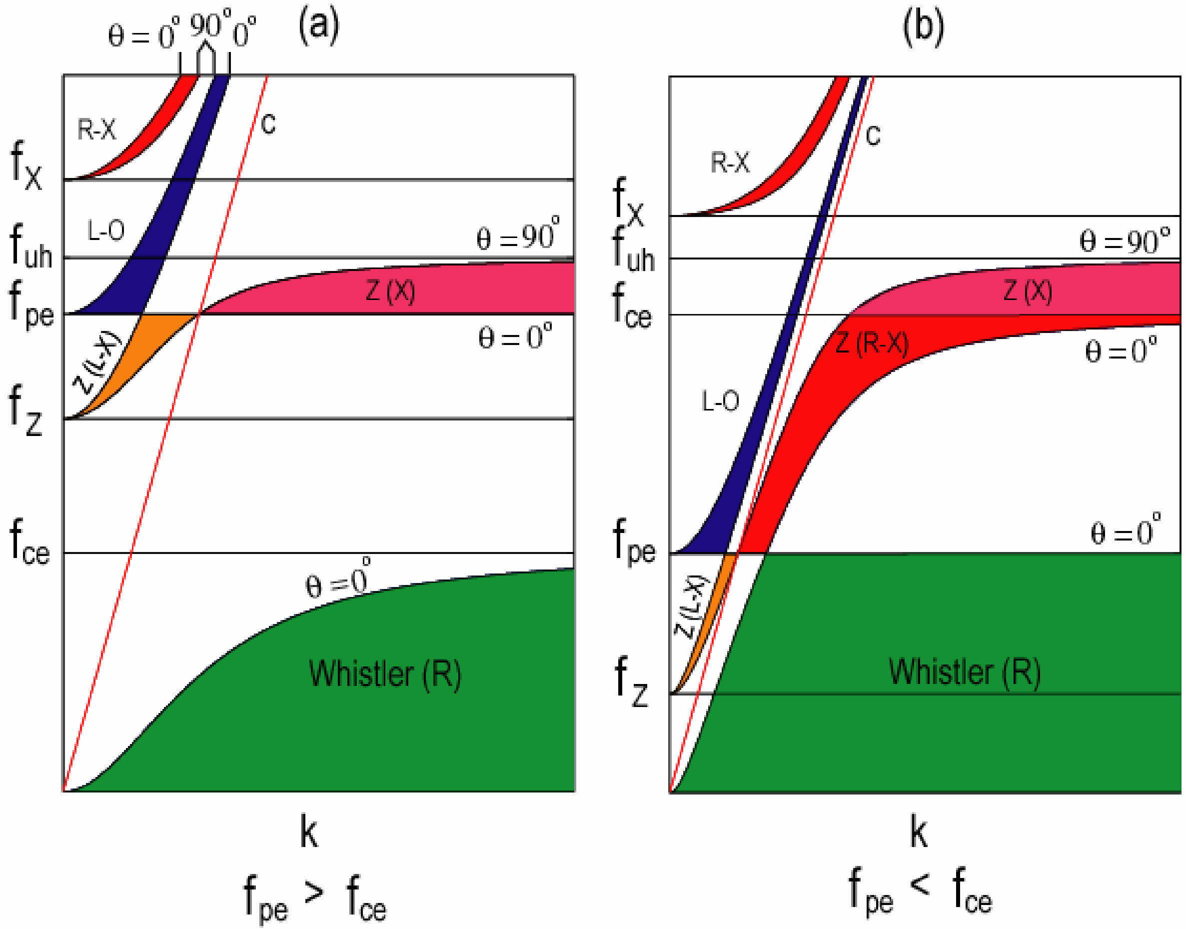

1. R-X reflects at f_R

L-O Reflects at f_{pe}

Z reflects at f_Z or f_{pe}

WM reflects at $f=f_{lh}$
(Ion effects)
and at Earth-Ionosphere Boundary
(Measurement below F2 peak)

2. WM is a slow wave mode

Large Refractive index: 1-10,000

Small Group Velocity: < c/10 to c/10000

High spatial resolution + Measurement of Irregularity ⟵

Advantages of Whistler Mode Sounding over R-X, L-O, and Z-mode Sounding

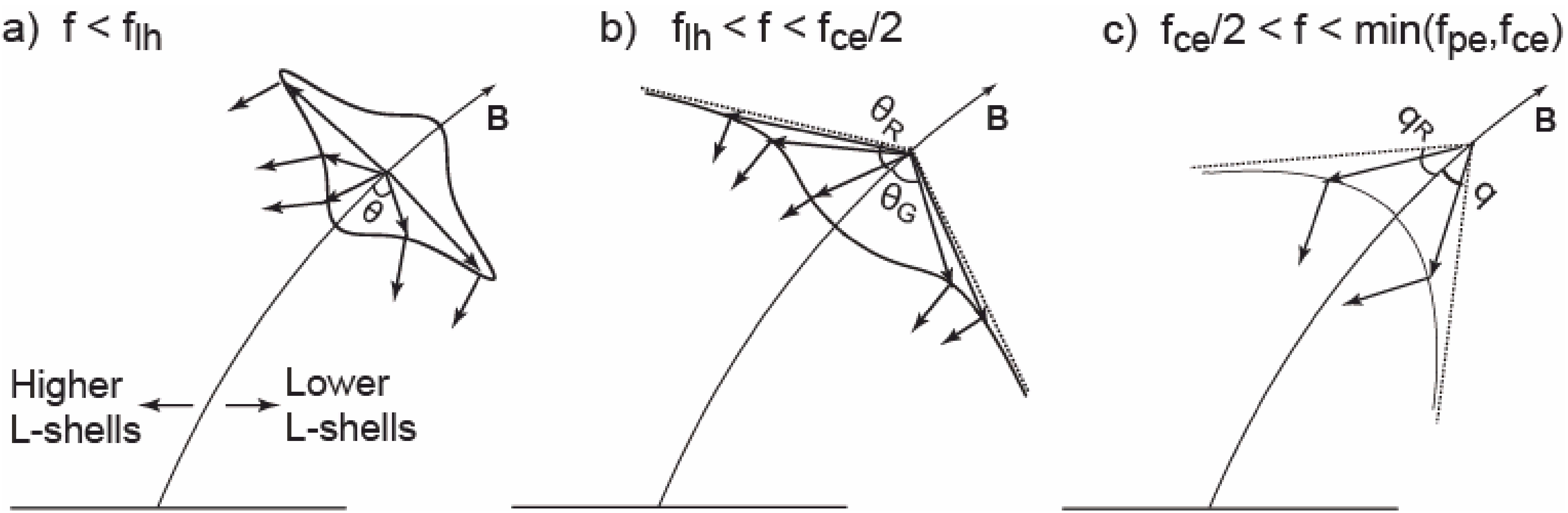

3. Whistler mode refractive index surface topology and size changes with frequency and the location on the field line $\longrightarrow$

Snell's Law leads to magnetospheric reflection and change of direction

4. WM waves propagate close to B

RPI/IMAGE active and passive experiments

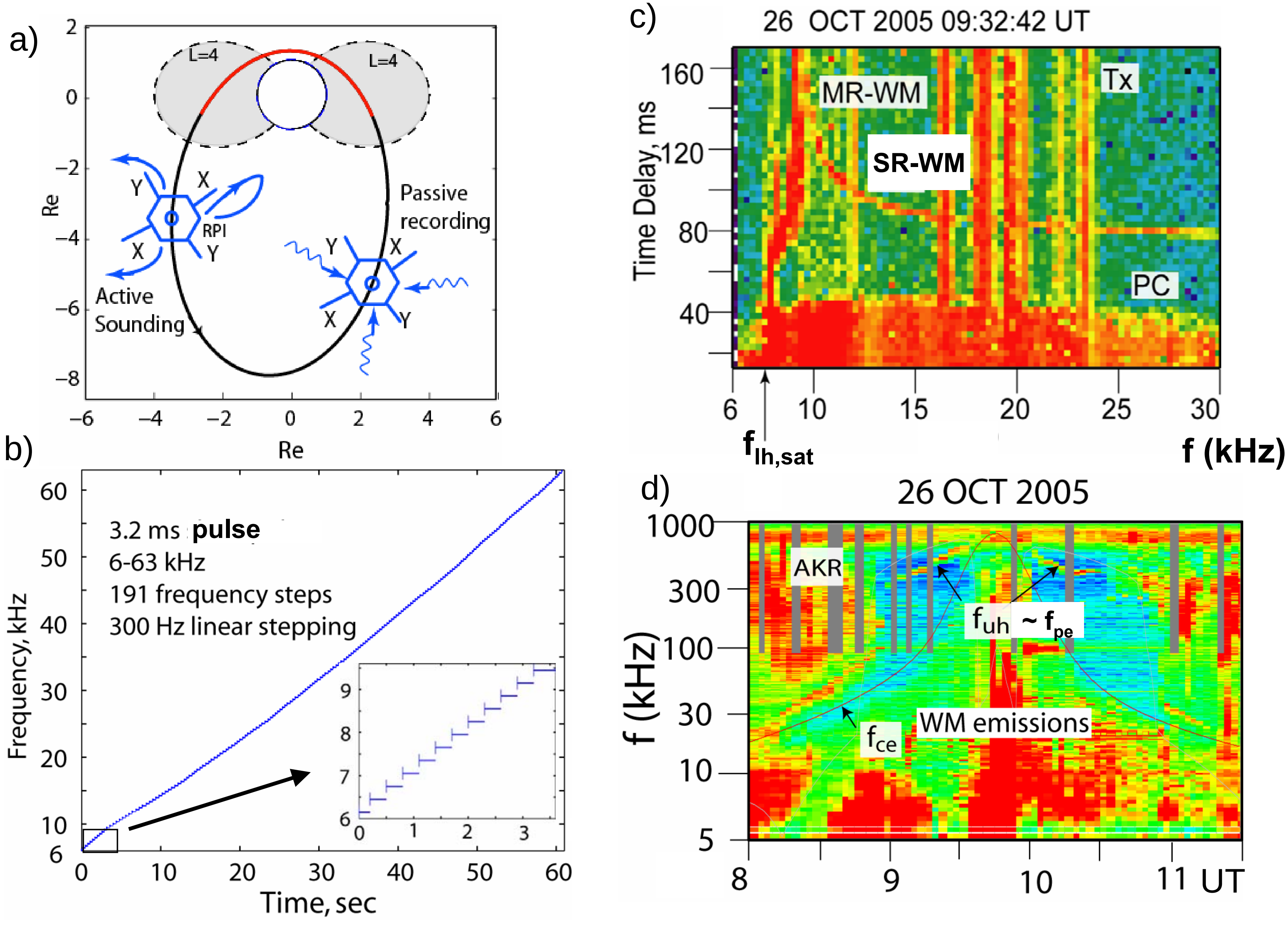

Whistler Mode Wave Reflection Mechanisms: Magnetospheric Reflection* (MR) and Specular Reflection (SR)

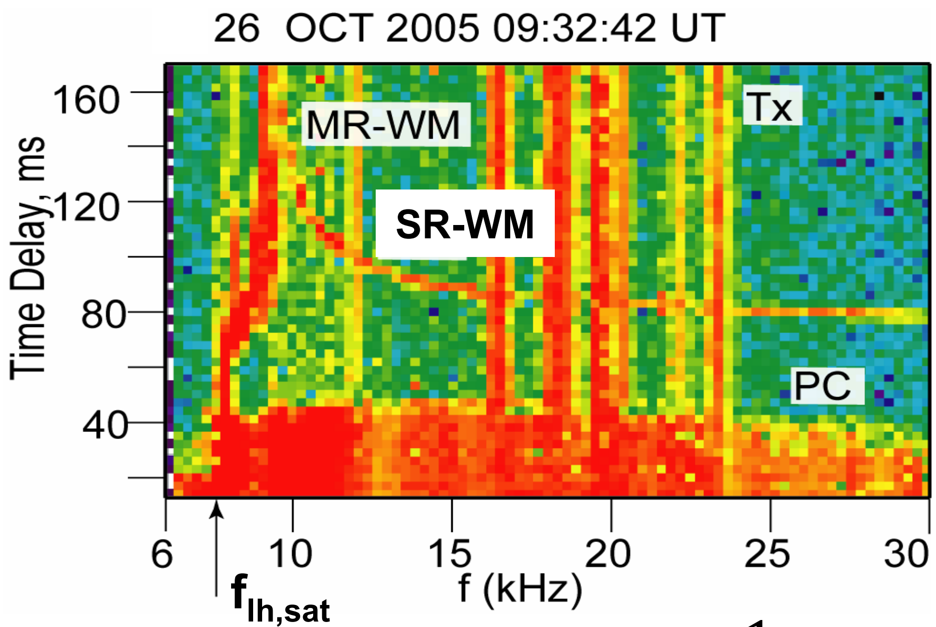

b) **SR-WM Echo**

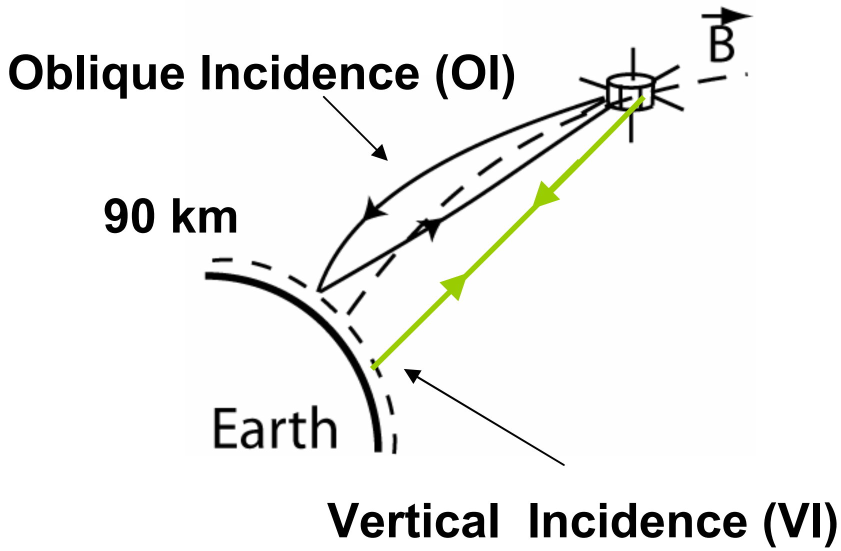

a) **MR-WM Echo**

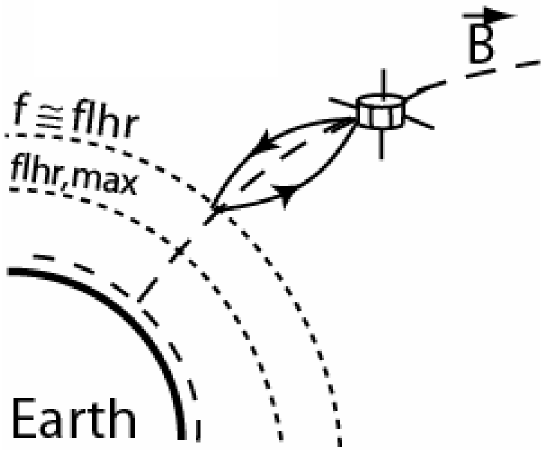

$$\frac{1}{meff}\frac{1}{(1836\, f_{lhr}{}^{2})} = \frac{1}{f_{pe}{}^{2}} + \frac{1}{f_{ce}{}^{2}}$$

$$\frac{1}{meff} = \frac{\alpha_{H^+}}{1} + \frac{\alpha_{He^+}}{4} + \frac{\alpha_{O^+}}{16}$$

*Kimura (1966), Radio Sci., 1 (3).

MR-WM Echo Generation Mechanism

$$\frac{1}{meff}\,\frac{1}{(1836\, f_{lhr}{}^{2})} = \frac{1}{f_{pe}{}^{2}} + \frac{1}{f_{ce}{}^{2}}$$

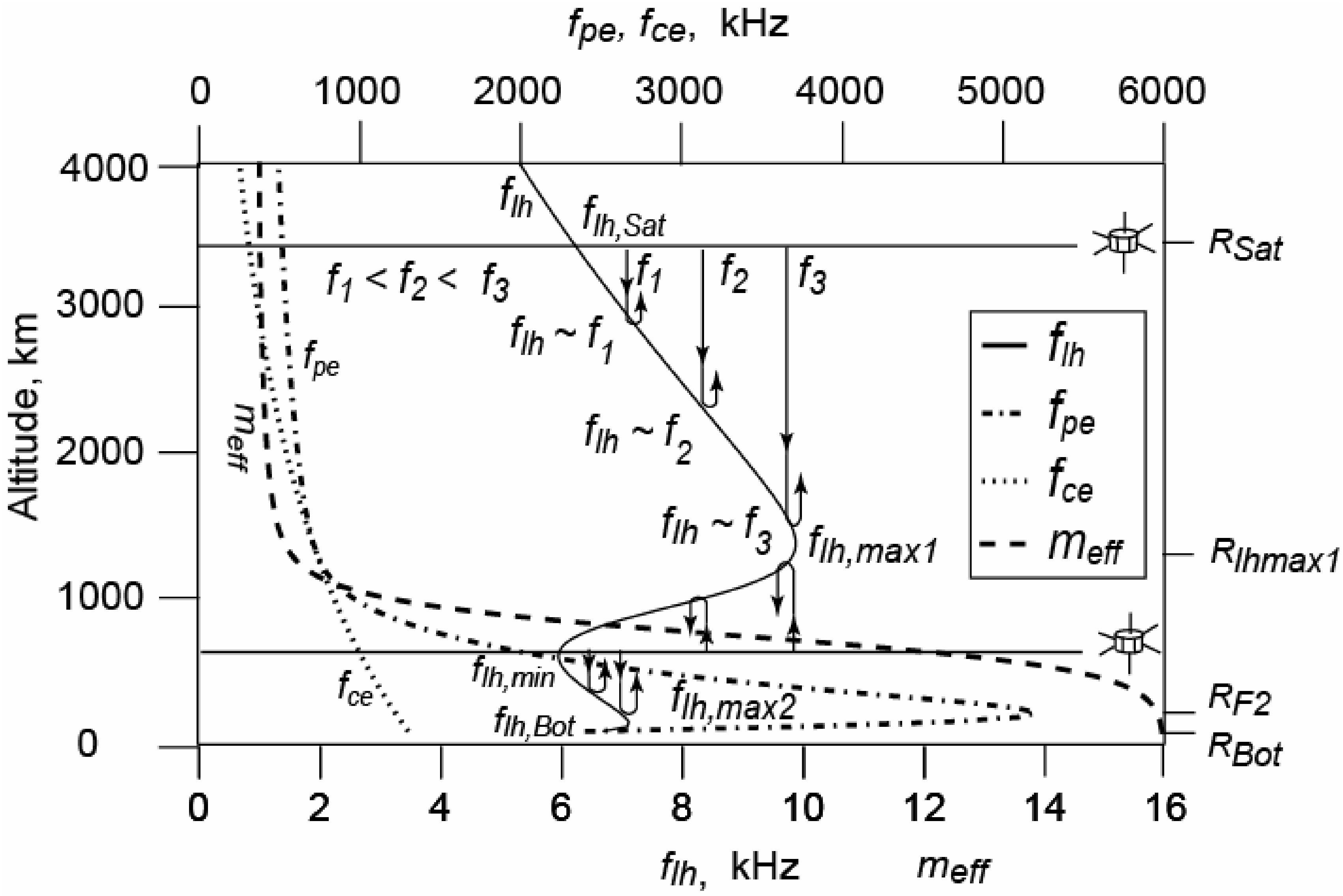

Types of SR-WM Echoes and Their Generation Mechanisms*

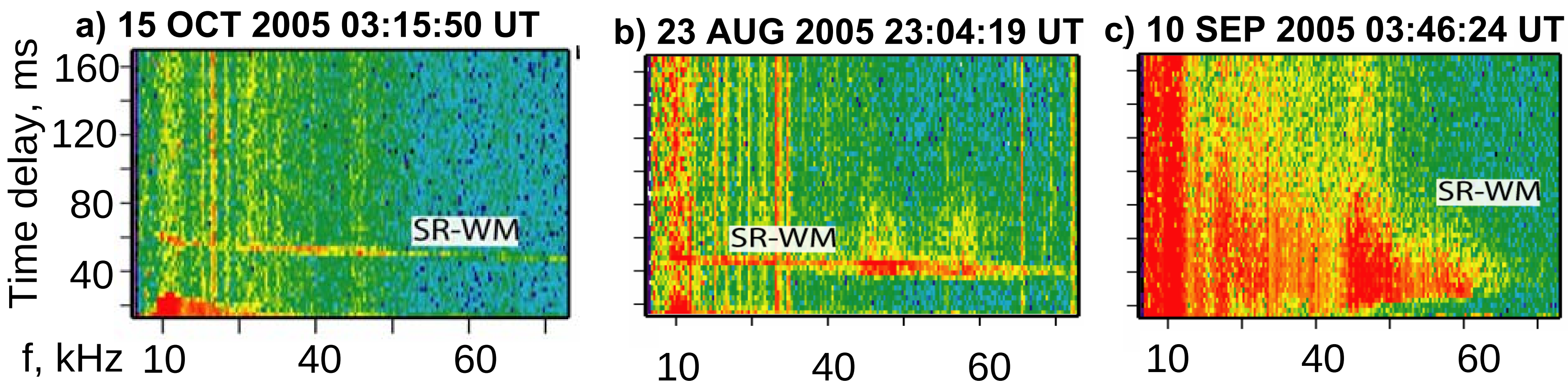

Discrete SR-WM echo

Multipath SR-WM echo

Diffuse SR-WM echo

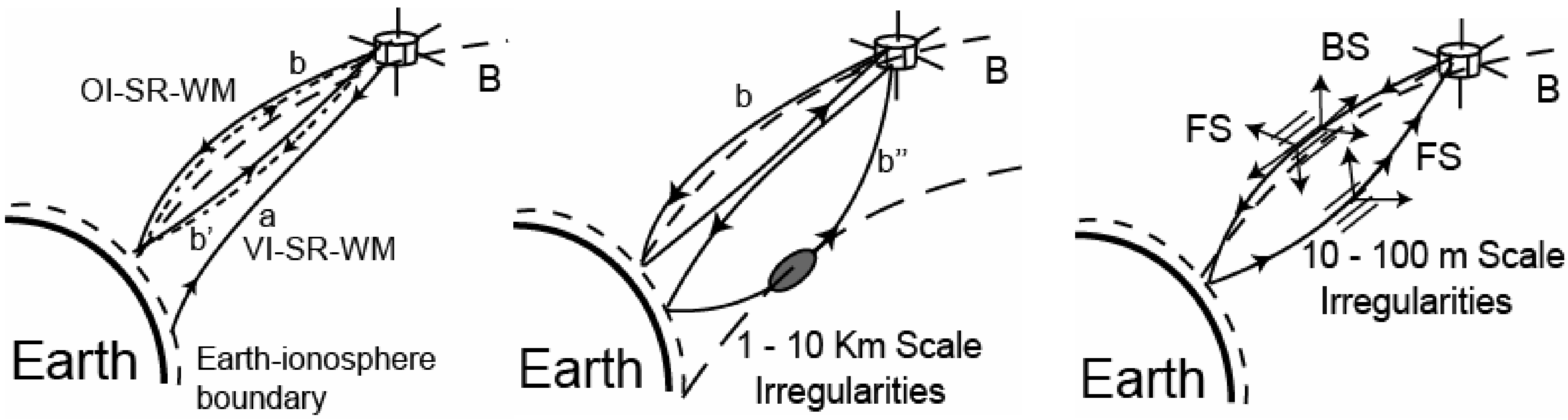

*Sonwalkar et al. (2004), *JGR*, 109, A11212

Types of MR-WM Echoes and Their Generation Mechanisms

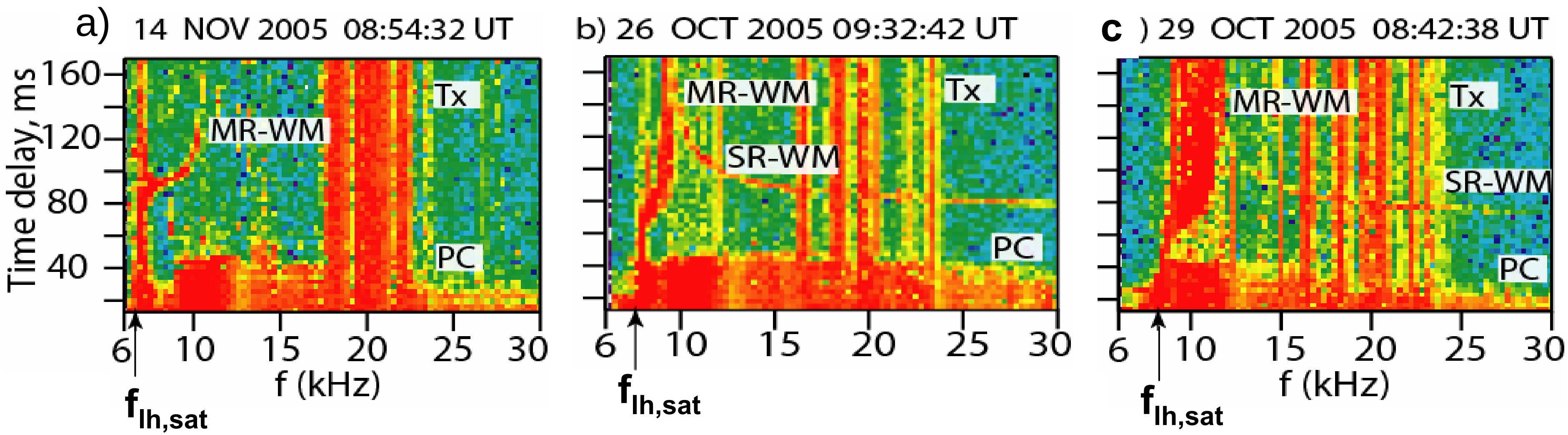

Discrete MR-WM Echo

Multipath MR-WM Echo

Diffuse MR-WM Echo

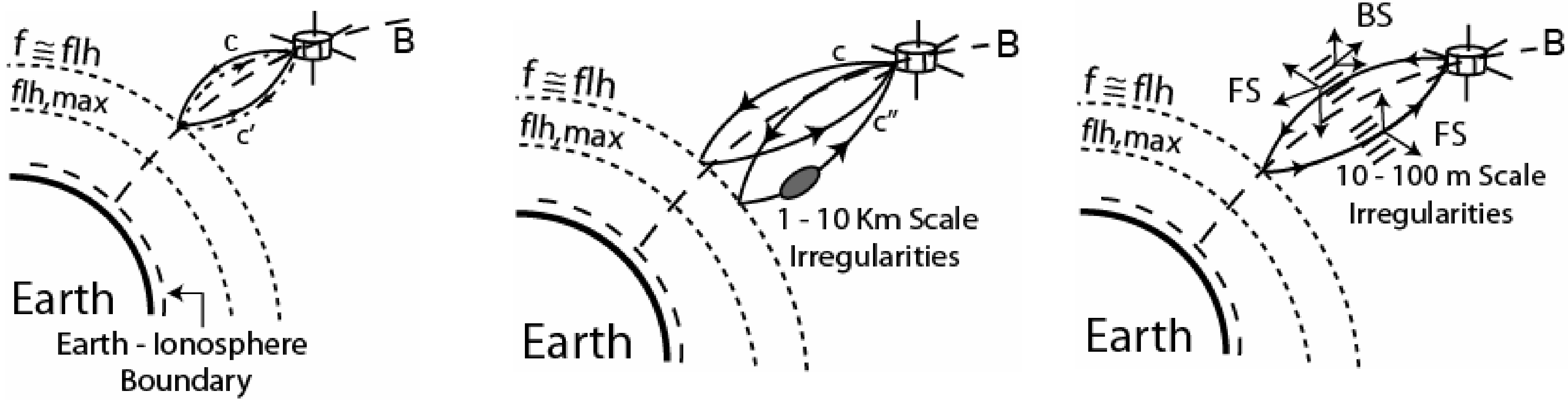

Occurrence Patterns of Whistler Mode Echoes

Both SR and MR are found on 20-25% of transmissions

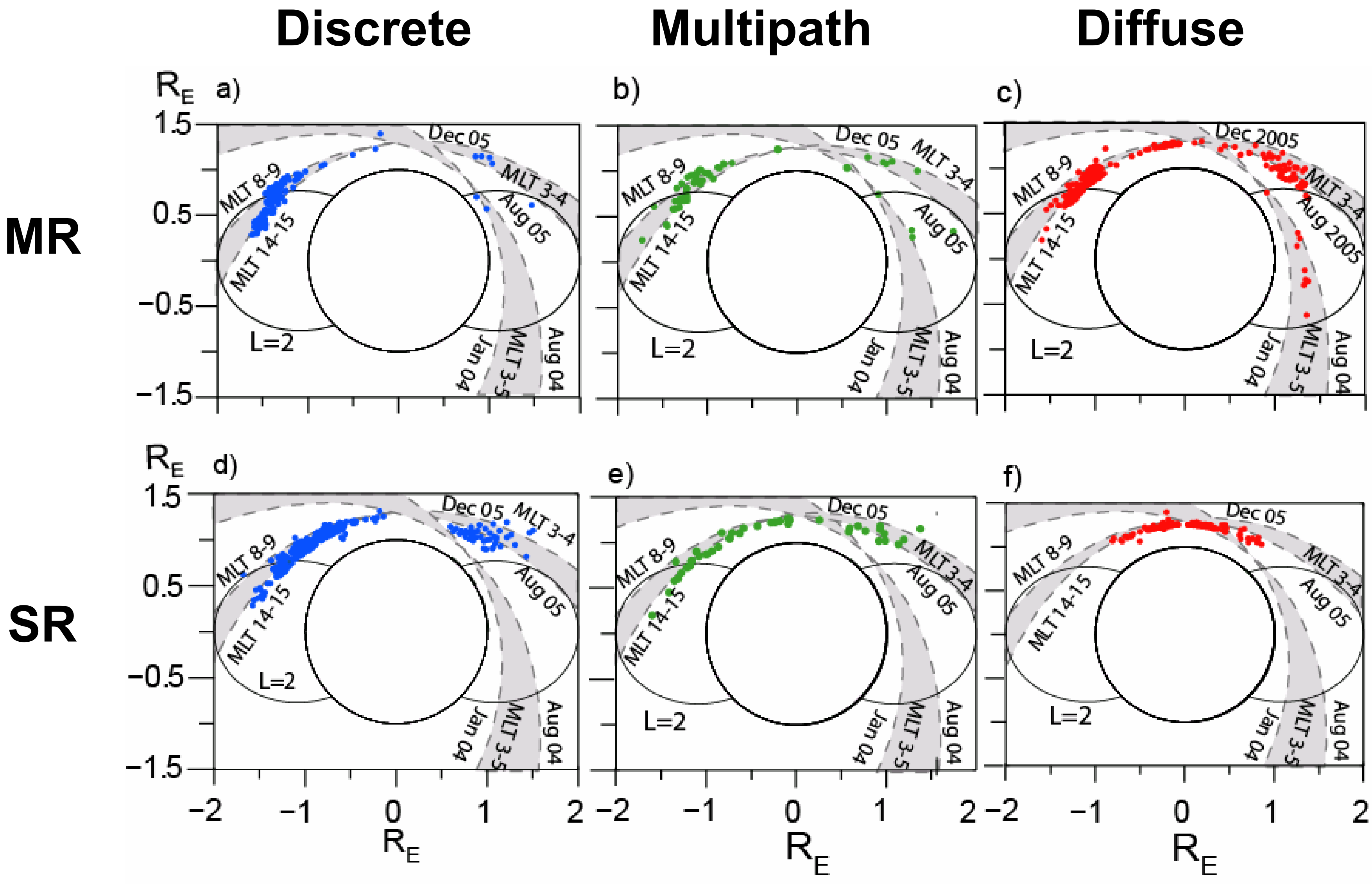

Ray tracing Analysis: Whistler Mode Sounding of e-, H+, He+, O+

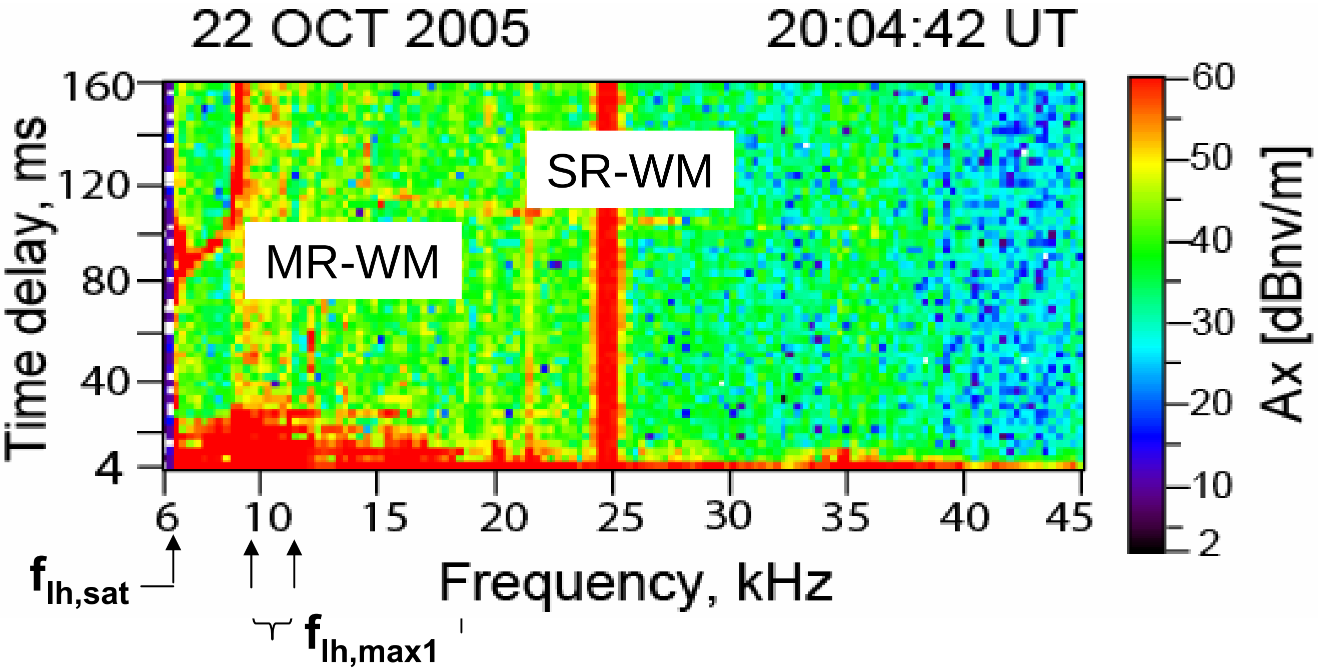

Measured Paramters:

$f_{lh,sat}$ $f_{lh,max1}$

t_g – f for MR-WM

t_g – f for SR-WM

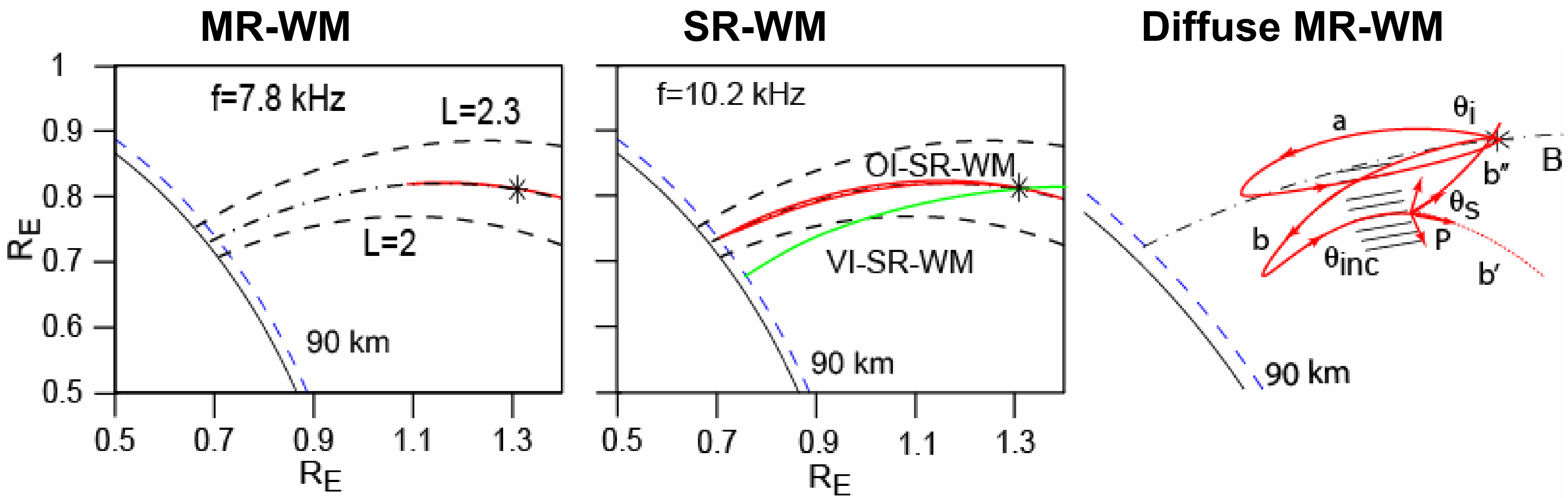

Ray Tracing Density Model: Diffusive Equilibrium

Thomas and Angerami (1964), *JGR*, 69, 4537.

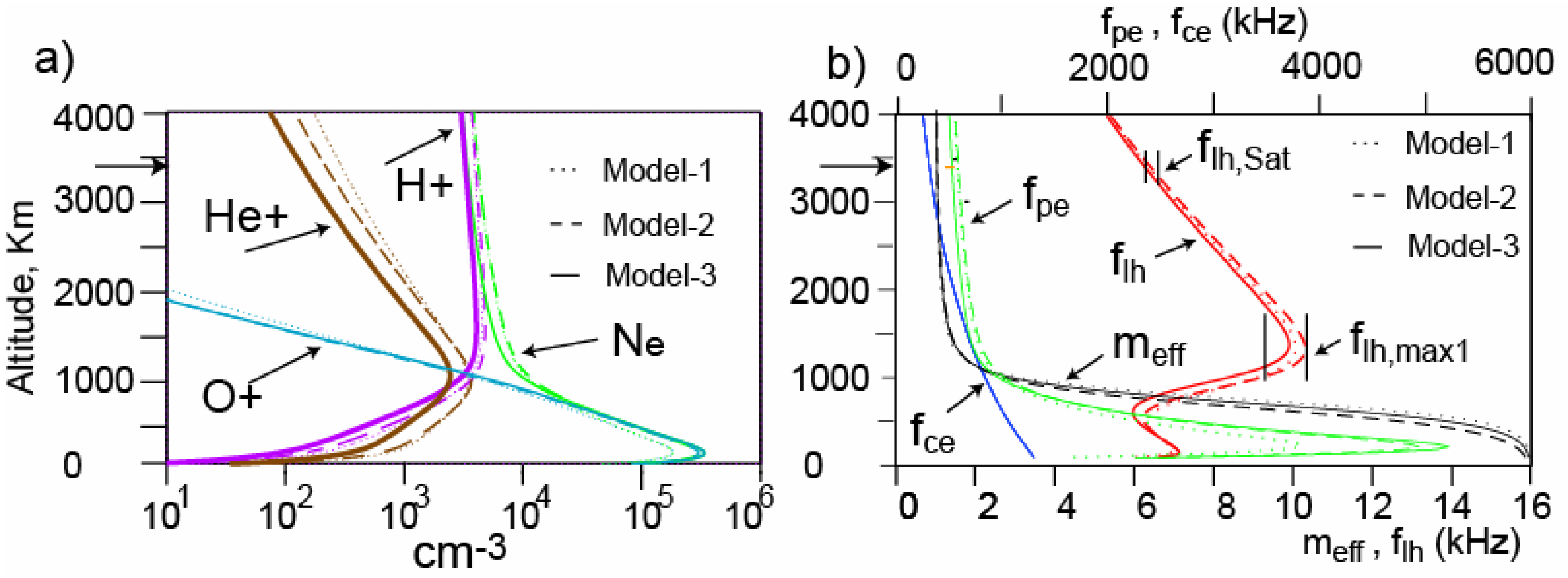

$$N_i = N_e \frac{\alpha_i e^{-\frac{r-r_b}{H_i}}}{\sum_{i=1}^{3} \alpha_i e^{-\frac{(r-r_b)}{H_i}}},$$

$$\frac{1}{meff}\frac{1}{(1836\, f_{lhr}{}^2)} = \frac{1}{f_{pe}{}^2} + \frac{1}{f_{ce}{}^2}$$

$$H_i = 1.1506(T)\left(\frac{r_b}{7370}\right)^2\left(\frac{r}{r_b}\right)\frac{1}{4^{(i-1)}}$$

$$\frac{1}{meff} = \frac{\alpha_{H^+}}{1} + \frac{\alpha_{He^+}}{4} + \frac{\alpha_{O^+}}{16}$$

i=1 → H+, i=2 → He+, i=3 → O+

Results of Ray Tracing: e-, H+, He+, and O+ densities along B

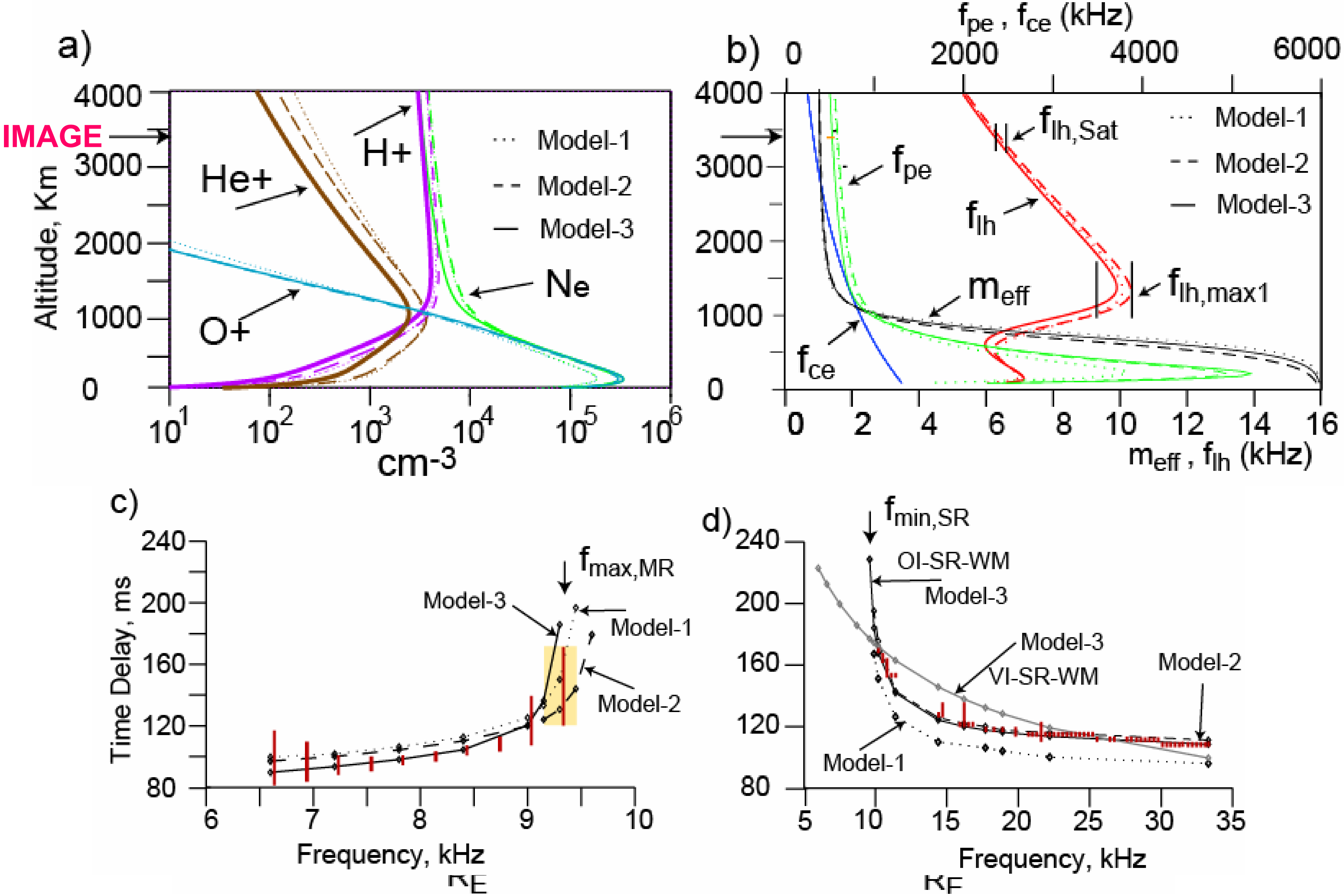

Summary & Conclusions

• MR- and SR-WM echoes in great variety were observed at < 5,000 km altitude, at all latitudes, and Kp.

• Introduced new method of WM radio sounding of N_e, N_{H+}, N_{He+}, N_{O+}, and FAI along **B.** Uncertainty in measurement ~10-20%; Resolution ~0.1 L
Electron and ion density measurements are consistent with past results (e.g. Clilverd et al., 2003; Craven et al., 1997; Brinton et al., 1969).

• Whistler mode radio sounding will lead to new empirical models of magnetospheric plasma (N_e , N_i , FAI) as functions of geophysical conditions for gaining new understanding of mechanisms important to magnetosphere-ionosphere coupling, and for use in space weather predictions.

• Analysis of whistler mode echoes will help in understanding the generation mechanisms of naturally occurring whistler mode waves (e.g. hiss and chorus).

• Analysis of WM echoes will lead to new understanding of the radiation and receiving properties of dipole antennas in a magnetoplasma.

SIGNIFICANCE OF THIS RESEARCH

- Radio sounding at < 5,000 km of electrons, ions, and FAI along **B**
- Gain new insight of ionosphere-magnetosphere coupling
- New understanding of generation mechanisms of hiss and chorus
- Radiation and receiving properties of dipole antennas at VLF

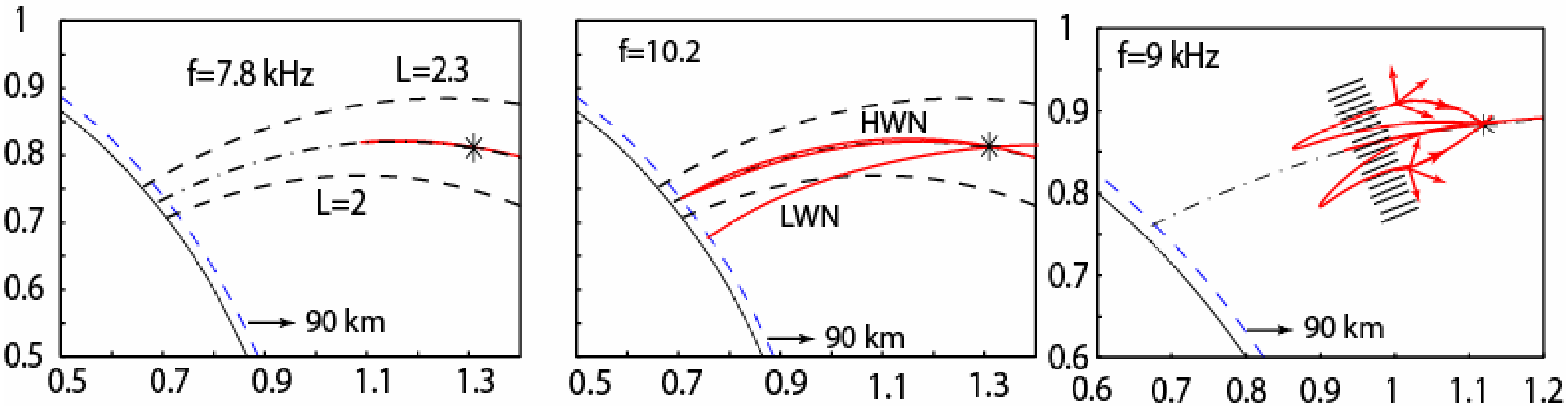

f=7.8 kHz
L=2.3
L=2
90 km
f=10.2
HWN
LWN
90 km
f=9 kHz
90 km

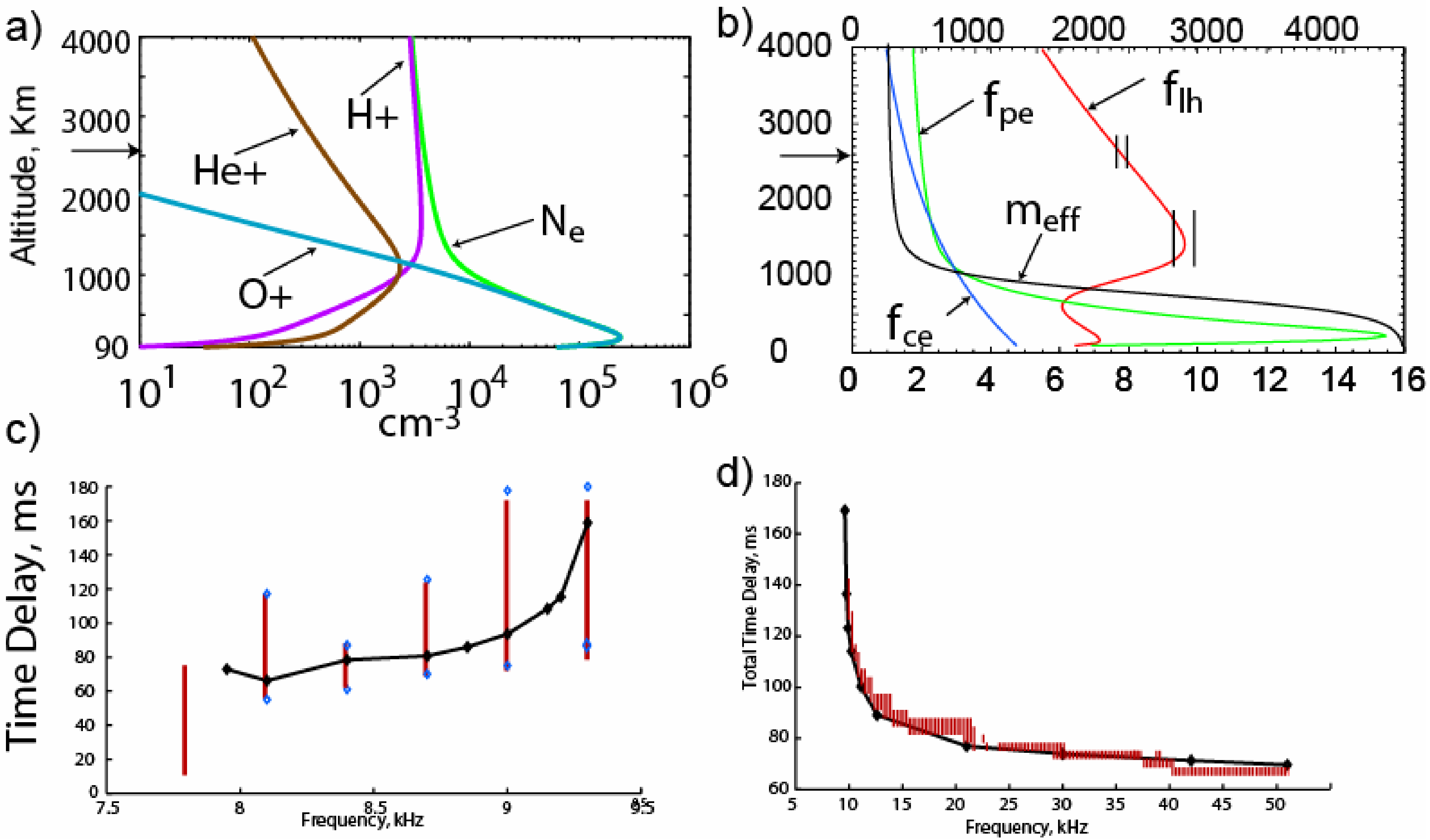

a)
Altitude, Km
4000
3000
2000
1000
90
He+
H+
O+
N_e
10^1 10^2 10^3 10^4 10^5 10^6
cm^{-3}
b)
0 1000 2000 3000 4000
f_{pe}
f_{lh}
m_{eff}
f_{ce}
0 2 4 6 8 10 12 14 16
c)
Time Delay, ms
Frequency, kHz
d)
Total Time Delay, ms
Frequency, kHz

Types of SR-WM Echoes and Their Occurrence Patterns

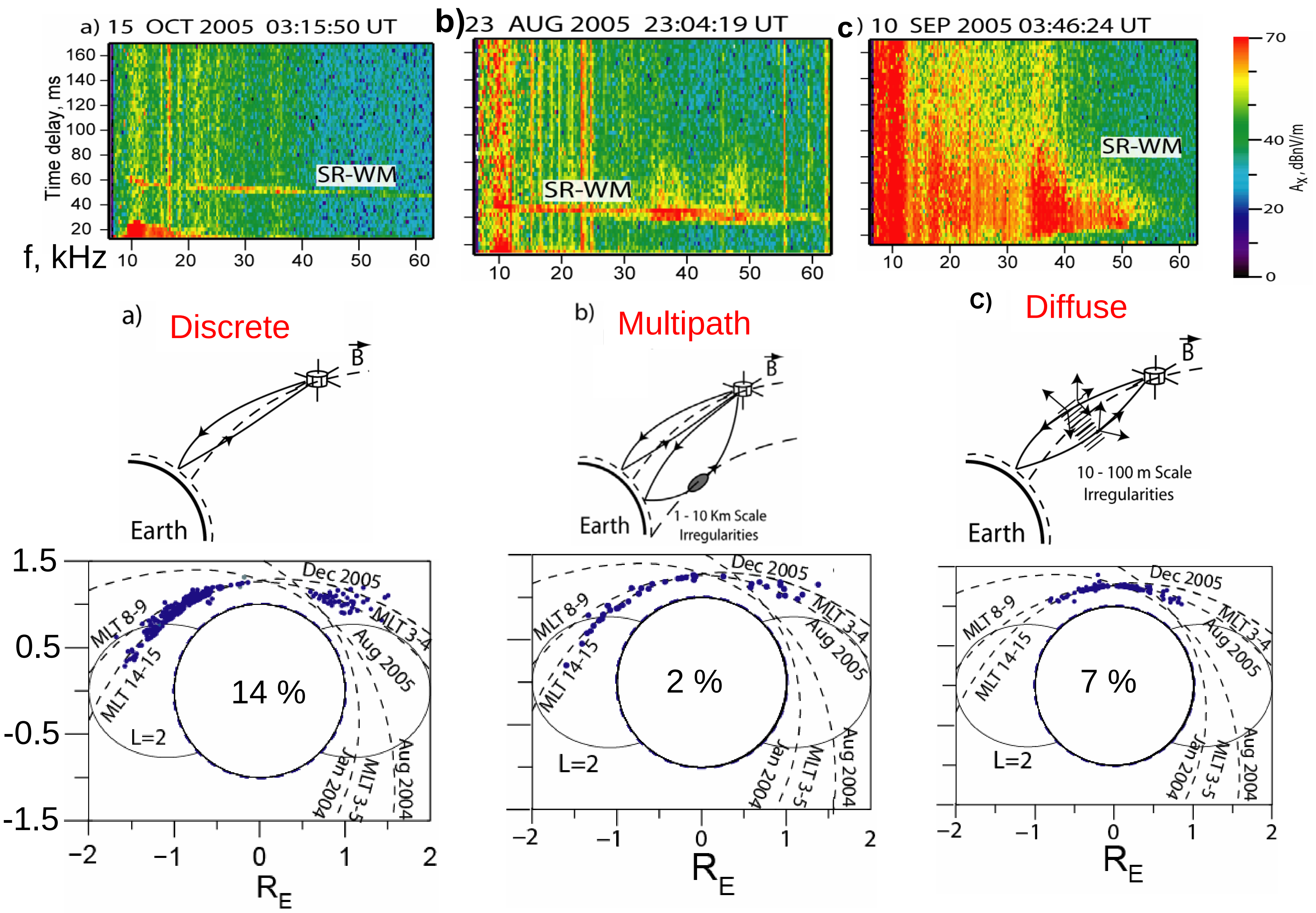

Types of MR-WM Echoes and Their Occurrence Patterns

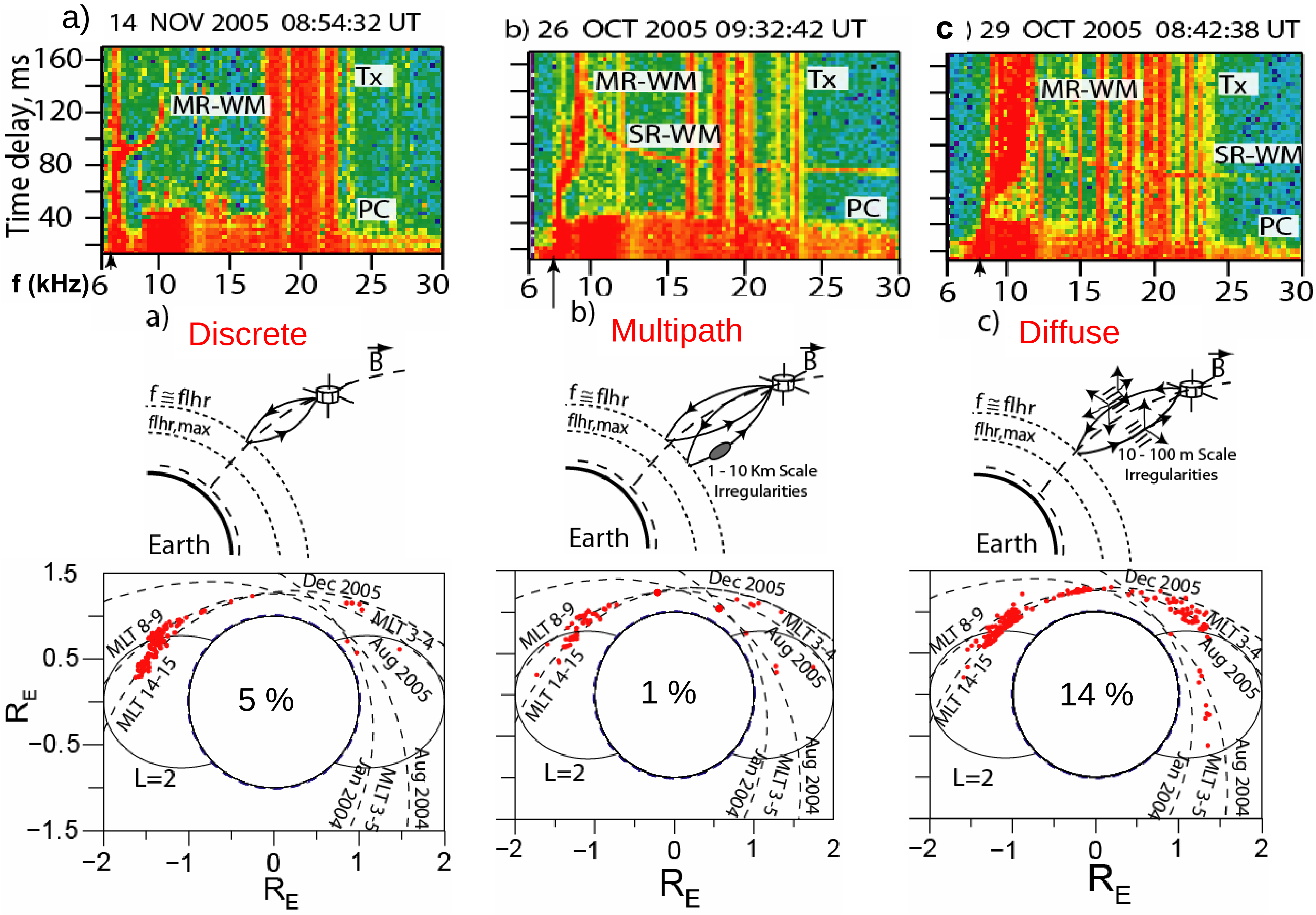

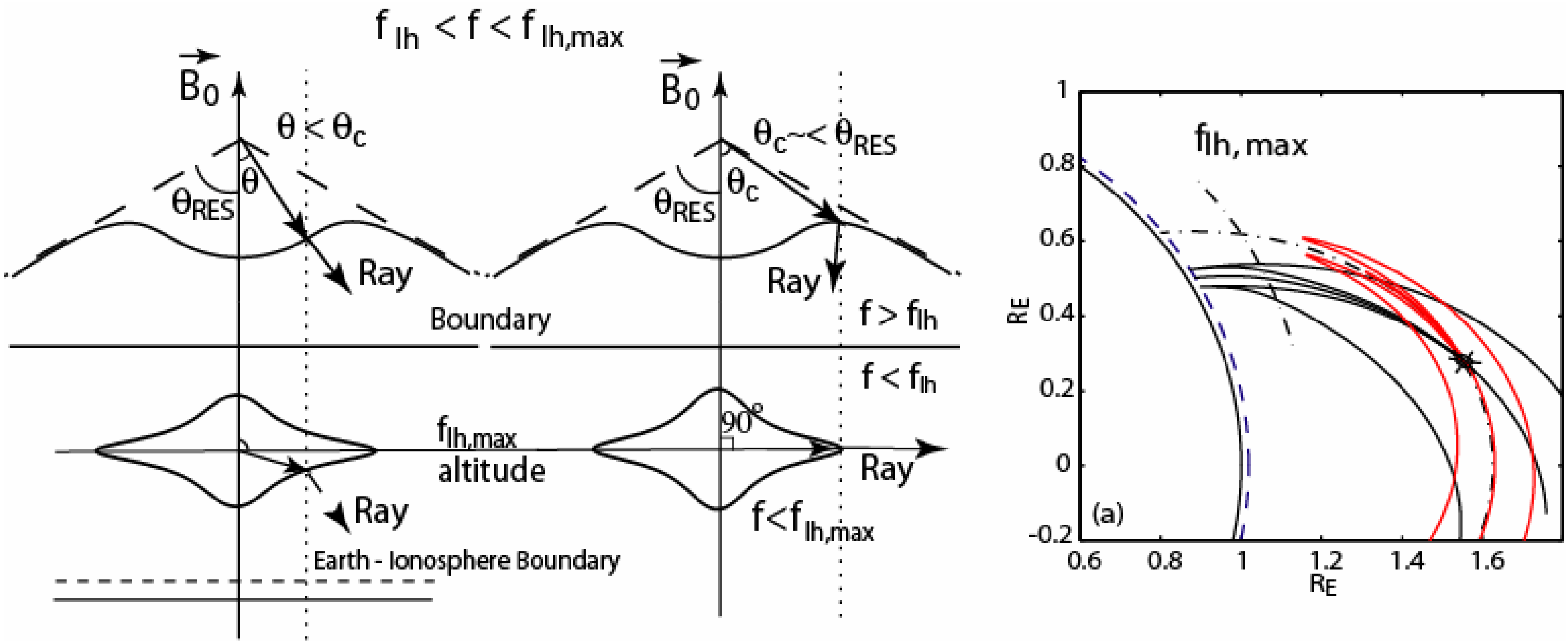

f lh < f < f lh,max
B0
θ < θc
θ
θRES
Ray
B0
θc~< θRES
θc
θRES
Ray
Boundary
f > flh
f < flh
flh,max
altitude
Ray
90°
Ray
f<flh,max
Earth - Ionosphere Boundary
flh, max
RE
RE
(a)
1
0.8
0.6
0.4
0.2
0
-0.2
0.6
0.8
1
1.2
1.4
1.6